Composites Science and Technology 70 (2010) 1242–1248

Contents lists available at ScienceDirect

Composites Science and Technology

journal homepage: www.elsevier.com/locate/compscitech

Synthesis and characterization of well-dispersed multi-walled carbon nanotube/low-bandgap poly(3,4-alkoxythiophene) nanocomposites

Cheng-Dar Liu [a], De-Yu Shu [b], Ching-Ting Tsao [a], Jin-Lin Han [c], Feng-Yu Tsai [a,d], Fang-Chung Chen [e], Wen-Chang Chen [a,b], Kuo-Huang Hsieh [a,b,*]

[a] Institute of Polymer Science and Engineering, National Taiwan University, Taipei 106, Taiwan
[b] Department of Chemical Engineering, National Taiwan University, Taipei 106, Taiwan
[c] Department of Chemical and Material Engineering, National ILan University, I-Lan 260, Taiwan
[d] Department of Material Science and Engineering, National Taiwan University, Taipei 106, Taiwan
[e] Department of Photonics, National Chiao-Tung University, Hsinchu 300, Taiwan

ARTICLE INFO

Article history:
Received 25 August 2009
Received in revised form 5 February 2010
Accepted 20 March 2010
Available online 27 March 2010

Keywords:
A. Carbon nanotubes
A. Polymer–matrix composites (PMCs)
D. Raman spectroscopy
D. Scanning electron microscopy (SEM)
D. Transmission electron microscopy (TEM)

ABSTRACT

In this study, we prepared nanocomposites of multi-walled carbon nanotubes (MWCNTs) and low-energy-bandgap conjugated polymers incorporating 3,4-alkoxythiophene monomers. Poly(3,4-dihexyloxythiophene) (PDHOT) and poly(3,4-dimethoxythiophene-*co*-3,4-dihexyloxythiophene) [P(DMOT-*co*-DHOT)] have relatively low-energy-bandgaps (ca. 1.38 and 1.34 eV, respectively), determined from the onsets of absorbances in their UV–Vis spectra, because of the electron-donating effects of their alkoxy groups. MWCNTs have poor solubility in common organic solvents; after surface modification with alkyl side chains using the Tour reaction, however, the *p*-hexylaniline modified MWCNT derivative (MWCNT-HA) was readily dispersed in $CHCl_3$ and could be mixed with the low bandgap polymers. Scanning electron microscopy images revealed that MWCNT-HA was dispersed well in each polythiophene derivative; only a few MWCNT-HA bundles could be observed at a high MWCNT-HA content (≧20 wt.%). The electrical conductivities of the MWCNTs/PDHOT composites were dependent on their MWCNT content, reaching 16 S/cm at 30 wt.% MWCNT-HA. We suspect that the two hexyloxy chains of PDHOT enhanced its solubility and allowed it to wrap around the surfaces of the MWCNTs more readily.

1. Introduction

Conjugated polymers (CPs) are used extensively in functional materials because of their interesting optical, electrical, and redox properties. The properties of CPs depend mostly on the energy of their bandgaps (E_g), defined as the difference in energy between the highest occupied molecular orbital (HOMO) and lowest unoccupied molecular orbital (LUMO). There is great interest in the application of low-energy-bandgap materials in polymer light-emitting diodes (PLEDs), organic thin-film transistors (OTFTs), optical transparent electrodes, and organic photovoltaics (OPVs) [1,2]. By definition, a low-energy-bandgap polymer is a conjugated polymer having a value of E_g of 1.5 eV or less, with the onset of its absorption at a wavelength of 600 nm or greater in the neutral state, as measured using UV–Vis spectroscopy [3,4]. In early studies, the bandgap energy was found to be strongly correlated with the molecular geometry. For example, polythiophene, with its aromatic geometry, has a calculated bandgap energy of 2 eV; the structurally similar quinoid isomer has a value of only 0.47 eV [5]. Wudl et al. synthesized polyisothianaphthene (PITN), which has a bandgap energy of 1.13 eV as a result of the preferred stabilization of the quinoid resonance from the benzene ring. Chen and Jenekhe synthesized many soluble conjugated poly(heteroarylene methines) that have low bandgap energies (ca. 1.14 eV) [6–8]. Furthermore, Sotzing and co-workers reported that the value of E_g of polythieno[3,4-b]furan is 1 eV [9]. At present, derivatives of polythiophene (PT) and its copolymers are the hottest candidates for developing new low-energy-bandgap materials.

The use of carbon nanotubes (CNTs) in polymer/CNT composites has become a focal point of nanocomposite research ever since Iijima's discovery of multi-walled carbon nanotubes (MWCNTs) [10]. Because CNTs possess high surface areas, chemical stability, high electrical conductivity [11], low mass density, and good mechanical strength [12], they have been developed for application in several fields, including chemical detectors, supercapacitors [13], electromagnetic interference (EMI) materials [14], and transparent electrodes [15]. In addition, composites of CNTs and CPs have also been employed widely in OTFTs and OPVs in recent years [16]

* Corresponding author at: Institute of Polymer Science and Engineering, National Taiwan University, No. 1, Sec. 4, Roosevelt Rd., Taipei 10617, Taiwan. Tel.: +886 2 33665314; fax: +886 2 33665237.
E-mail address: khhsieh@ntu.edu.tw (K.-H. Hsieh).

0266-3538/$ - see front matter © 2010 Elsevier Ltd. All rights reserved.
doi:10.1016/j.compscitech.2010.03.012

because the high charge mobilities, long conjugation lengths, and large aspect ratios of CNTs are favorable properties for charge transfer [17]. The advantages of CNTs are, however, usually offset by their insolubility and poor dispersibility in polymer matrices. The performances of such composites depend on not only the properties of the components but also their arrangement in the matrix [18,19]. As a result, many surface modification techniques have been used to improve the solubility of CNTs in solvents and matrixes [20]. Among them, the Tour reaction is one of the most accommodating and directly applicable methods for modifying the surface of CNTs. Tour and co-workers initially employed a reduced aryl diazonium salt to give an aryl radical for covalent attachment to the carbon surface. In a following report, they found that this reaction could be performed using derivatives of aniline treated with alkyl nitrites to achieve functionalization of up to 1 in 20 carbon atoms in the CNT framework without via chemistry on the ends of the cut nanotube [21].

In this paper, we report the synthesis of two soluble low-E_g PT derivatives: poly(3,4-dihexyloxythiophene) (PDHOT) and poly(3,4-dimethoxythiophene-*co*-3,4-dihexyloxythiophene) [P(DMOT-*co*-DHOT)]. We mixed them with the *p*-hexylaniline modified MWCNT derivative (MWCNT-HA) which we fabricated using the Tour reaction, a simple transformation that results in relatively little damage to the CNTs. We used scanning electron microscopy (SEM) to investigate the morphologies of the dispersions of these MWCNTs in matrices of the PT derivatives, and determined their electrical conductivities.

2. Experimental

2.1. Materials

3,4-Dimethoxythiophene (DMOT) was purchased from Aldrich; other chemicals used to synthesized 3,4-dihexyloxythiophene (DHOT) were purchased from ACROS. Poly(3-hexylthiophene-2,5-diyl) (P3HT, M_w 45,000–65,000 g/mol) was purchased from Aldrich; its regioregularity was greater than 99.995%. MWCNTs (CP-181) were obtained from Advance NanoPower, Taiwan, and purified using 5 N $HCl_{(aq)}$ to remove residual Fe catalyst.

2.2. 3,4-Dihexyloxythiophene (DHOT) [22]

A mixture of DMOT (3.4 g), hexanol (5.31 g), and *p*-toluenesulfonic acid monohydrate (0.41 g) in dry toluene (140 mL) was stirred for 72 h under reflux. After quenching the reaction with cool water, the mixture was extracted with CH_2Cl_2. The organic layer was collected, dried ($MgSO_4$), and evaporated to yield a black liquid, which was purified through column chromatography (CH_2Cl_2/hexane, 1:20) to obtain DHOT as a transparent liquid (75%). ^{1}H NMR ($CDCl_3$): δ 6.1 (s, 2H, ThH_2), 3.9 (s, 4H, OCH_2), 1.6–1.8 (m, 4H, CH_2), 1.2–1.4 (m, 12H, CH_2), 0.9 (s, 6H, CH_3).

2.3. Polymerization of PDHOT and P(DHOT-co-DMOT)

A solution of monomers (0.2 g) dissolved in dry $CHCl_3$ (7 mL) was added dropwise to $FeCl_3$ (4 equiv.). The mixture was stirred for 24 h at ambient temperature and then subjected to Soxhlet extraction with MeOH for 24 h. The precipitate was then washed through Soxhlet extraction with CH_2Cl_2. The filtrate was dried under vacuum to yield a dark pink polymer. Dedoped polymers were obtained after stirring the polymers in 10% aqueous NH_4OH (100 mL) for 24 h.

2.4. Alkyl-modified MWCNT-HA [21]

Pristine MWCNT (40 mg) and *p*-hexylaniline (2.364 g) were mixed in a flask equipped with a reflux condenser and a magnetic stirrer bar. After heating to 80 °C, isoamyl nitrite (2.152 g) was added via syringe and the mixture stirred vigorously for 2 h. The contents were diluted with acetone (150 mL) and passed through a PVDF filter (0.47 μm). The filter cake was washed with deionized water and acetone until the filtrate was clear. The final product was dried in an oven at 80 °C for 24 h.

2.5. MWCNT/PT derivative composites

The MWCNTs were added to $CHCl_3$ to give a concentration of 1 mg/mL; the mixture was subjected to sonication in a bath for 3 h to disperse the MWCNTs in the solvent. On the basis of the desired weight fraction of MWCNTs in the final composite, an appropriate quantity of the PT derivative doped with dodecylbenzenesulfonic acid (DBSA) was dissolved in the MWCNT/$CHCl_3$ mixture.

2.6. Characterization

SEM was conducted using a JEOL 6700 instrument operated at an accelerating voltage of 50 kV. Each sample was cleaved in liquid N_2 and its fresh fracture surface sputtered with gold. Transmission electron microscopy (TEM) was performed using a JEOL 1230 instrument operated at an accelerating voltage of 100 kV; the sample for imaging was prepared by placing a drop of the MWCNT suspension on a 200-mesh copper grid featuring a supporting carbon film. Raman spectra of solid samples were recorded using a HORIBA Jobin Yvon-iHR550 instrument, with excitation at 633 nm. The resistance of the material was measured using an HP4338B instrument. Testing films of each composite were manufactured through drop coating of five layers. Pristine MWCNT and MWCNT-HA samples were formed into powder-pressed pellets having a diameter of 1.26 cm and a thickness of ca. 0.1 cm. The final data were obtained from the average value of five measurements; the error range was less than 10%. The conductivity of material was calculated using the equation

$$\sigma = 1/Rd \quad (1)$$

where σ is the conductivity (in S/cm), R is the surface resistance (Ω/sq), and d is the thickness of the conductive film.

3. Results and discussion

Scheme 1a–c outlines the synthetic routes that we followed for the preparation of the monomers and polymers. DMOT was treated with hexanol under slightly acidic conditions in toluene at 110 °C; this transesterification reaction provided DHOT. Chemical polymerization of DHOT and DMOT was performed using $FeCl_3$. The reaction of DHOT itself resulted in a dark pink polymer, PDHOT, which was soluble in $CHCl_3$ and toluene and partially soluble in hot THF. The corresponding reaction of DMOT, with its shorter methoxyl side-chains, provided PDMOT, which was insoluble in any organic solvents and difficult to characterize. Therefore, we synthesized poly(DMOT-*co*-DHOT), using a feed molar ratio of DMOT to DHOT of 7:3; this copolymer was soluble in $CHCl_3$ when heated. The ^{1}H NMR spectrum of P(DMOT-co-DHOT) revealed (Fig. 1) one broad peak at ca. 1–1.83 ppm and another at 4.13 ppm. We attribute the former to the protons of the $(CH_2)_4CH_3$ group of DHOT and the latter from the protons of the OCH_2 group of DHOT and the OCH_3 group of DMOT. The molar ratio of DMOT to DHOT in the copolymer, which we estimated from the integrated

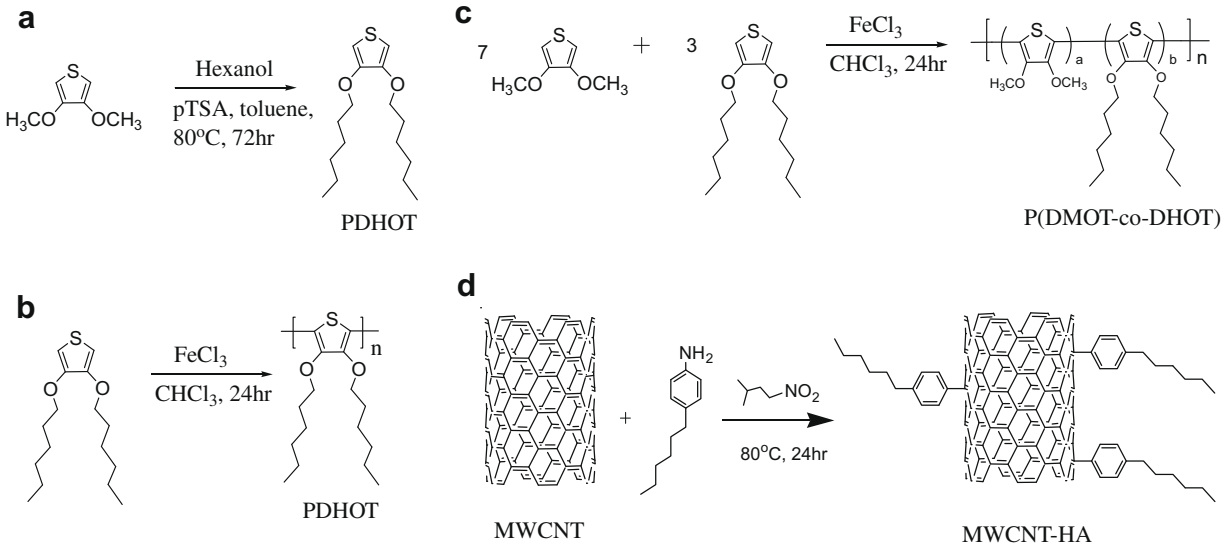

Scheme 1. (a)–(c) Synthetic procedures for the preparation of the monomers and polymers; (d) surface modification of a MWCNT using the Tour reaction.

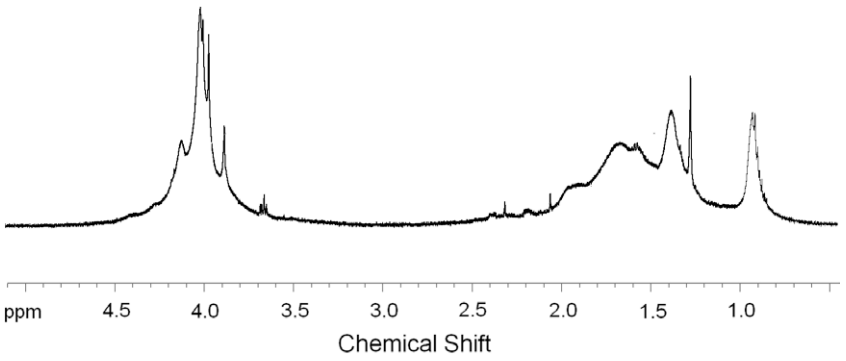

Fig. 1. ^{1}H NMR spectrum of P(DMOT-*co*-DHOT).

areas of these two broad peaks, was 1.64:1. This ratio is lower than the co-monomer feed ratio of 7:3 (i.e., 2.33:1).

Fig. 2 presents the UV–Vis absorption spectrum of each polymer diluted in $CHCl_3$; Table 1 summarizes the data. The spectra of PDHOT and P(DMOT-*co*-DHOT) featured similar peaks. P(DMOT-*co*-DHOT) displayed a π–π^* absorption band at a value of λ_{max} of 500 nm, blue-shifted by ca. 20 nm relative to that of PDMOT, and greater absorption intensity in the region 600–900 nm, presumably because the methoxyl groups on the thiophene unit made the backbone of the copolymer more rigid. Therefore, P(DMOT-*co*-DHOT) tended to form the quinoid type of PT and had the longer conjugated length. The presence of alkoxyl groups at the 3- and 4-positions of the thiophene rings provided PDHOT and P(DMOT-*co*-DHOT) with optical absorption maxima at longer wavelengths, with red-shifts in their values of λ_{max} of ca. 40–60 nm relative to that of P3HT. We attribute this behavior to the electron-donating effect of the alkoxyl groups and the more-coplanar conformation. As a result, PDHOT and P(DMOT-*co*-DHOT) possess low bandgap energies (ca. 1.38 and 1.34 eV, respectively), as determined from the onsets of the absorptions in their UV–Vis spectra.

Table 1
UV–Vis absorption and energy bandgap data for the PT derivatives.

Polymer	λ_{max} (nm)	Onset (nm)	E_g (eV)
PDHOT	520	900	1.38
P(DHOT-*co*-DMOT)	500	925	1.34
P3HT	460	580	2.14

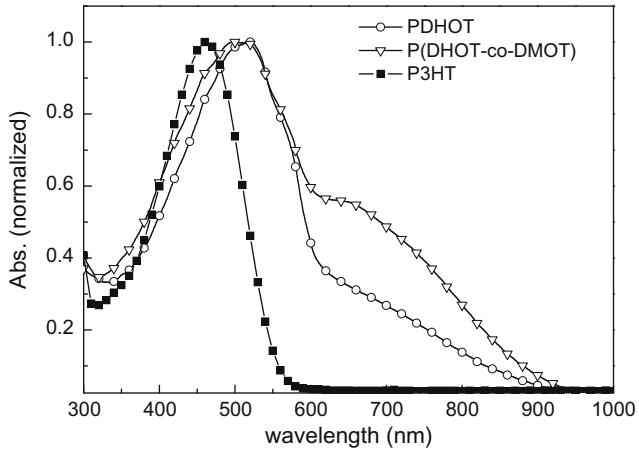

Fig. 2. UV–Vis absorption spectra of PDHOT, P(DHOT-*co*-DMOT), and P3HT.

Scheme 1d illustrates the surface modification of the MWCNTs using the Tour reaction. With this method, MWCNTs can be modified to present various functional groups (e.g., COOH, SO_3H, NO_2, alkyl chains) from appended aniline units. Because they are not

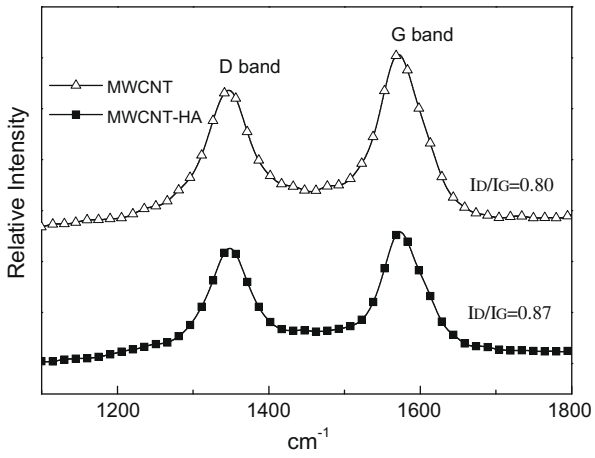

Fig. 3. Raman spectra of the pristine MWCNTs and MWCNT-HA.

treated with a 3:1 mixture of conc. H_2SO_4 and HNO_3, the MWCNTs are not cut and, therefore, they maintain their original aspect ratios. To allow the MWCNTs to disperse readily in organic solvents, we modified them with 4-hexylaniline. In this Tour reaction, 4-hexylaniline is converted into an aryl radical that becomes covalently attached to the MWCNT's surface, with the resulting presented hexylbenzene groups improving the solubility of the MWCNTs in $CHCl_3$. Fig. 3 reveals that, after the Tour reaction, significant changes occurred in the Raman absorption intensity within the region 1000–1800 cm^{-1}. Raman spectroscopy is a powerful tool for characterizing the presence of sp^2 and sp^3 hybridized atoms in the sidewalls of MWCNTs. The disorder band (D band) at ca. 1350 cm^{-1} represents C—C single bond linkages; the graphite bond (G band) at ca. 1580 cm^{-1} represents C=C double bonds. Fig. 3 reveals that MWCNT-HA features a higher ID/IG ratio (ca. 0.87) than that of the pristine MWCNTs (ca. 0.80), indicating successful functionalization.

We examined the stabilities of the pristine MWCNTs and MWCNT-HA in $CHCl_3$ through visual inspection (Fig. 4) and TEM analyses (Fig. 5). Samples of the pristine MWCNTs or MWCNT-HA (2.5 mg) were first dispersed in $CHCl_3$ (50 mL) under sonication for 1 h. When we removed the suspension of pristine MWCNTs from the bath, flocculation began to occur in the solvent during the first 10 min (Fig. 4a); after 24 h, a material slowly precipitated at the bottom of the vessel (Fig. 4b). In contrast, MWCNT-HA provided a well-dispersed solution in $CHCl_3$—one that did not provide any aggregation after 14 days (Fig. 4c). Fig. 5 presents TEM images of dried samples of the pristine MWCNTs and MWCNT-HA that had been dispersed in $CHCl_3$. The pristine MWCNTs appeared coiled and entangled because $CHCl_3$ is not a good solvent for them. The inset to Fig. 5a reveals that the average diameter of the pristine MWCNTs, estimated at a magnification of 200 k, was 15–25 nm. After functionalization with hexylbenzene groups, the product exhibited good solubility in $CHCl_3$; i.e., the coils of MWCNT-HA were more readily dismantled than those of the pristine MWCNTs.

Fig. 6a–c reveals that the three 20 wt.% MWCNTs/PT composites had similar morphologies, with macro-phase separation that fully filled with the pristine MWCNTs. Although π–π interactions be-

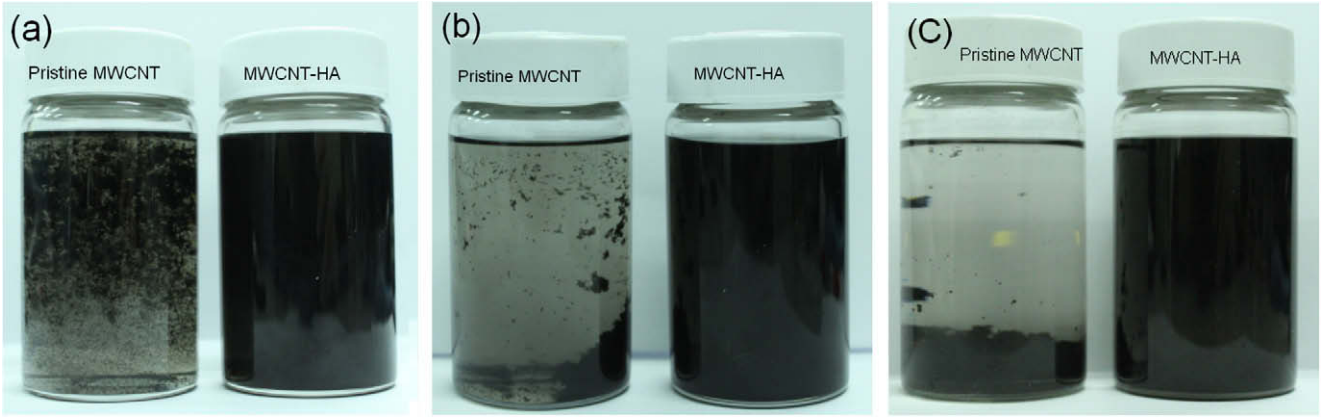

Fig. 4. Photograph displaying suspensions (2.5 mg/50 mL) of the pristine MWCNTs (left) and MWCNT-HA (right) in $CHCl_3$ after (a) 10 min, (b) 1 day and (c) 14 days.

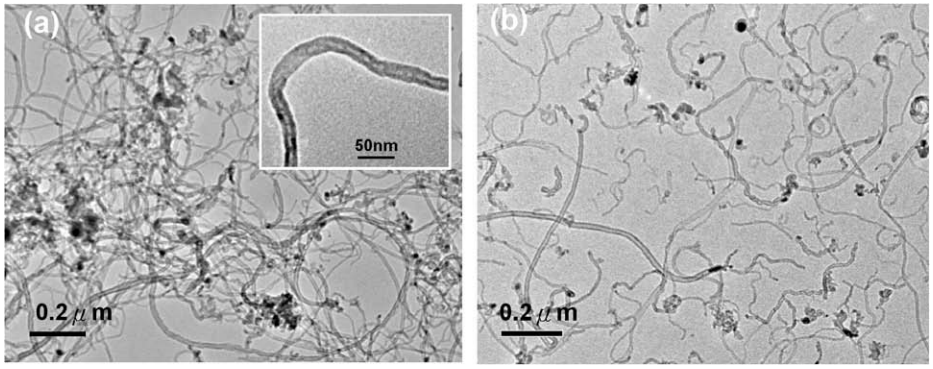

Fig. 5. TEM images of samples of: (a) the pristine MWCNTs and (b) MWCNT-HA obtained from their suspensions in $CHCl_3$. Inset: corresponding image of the pristine MWCNT sample at high magnification.

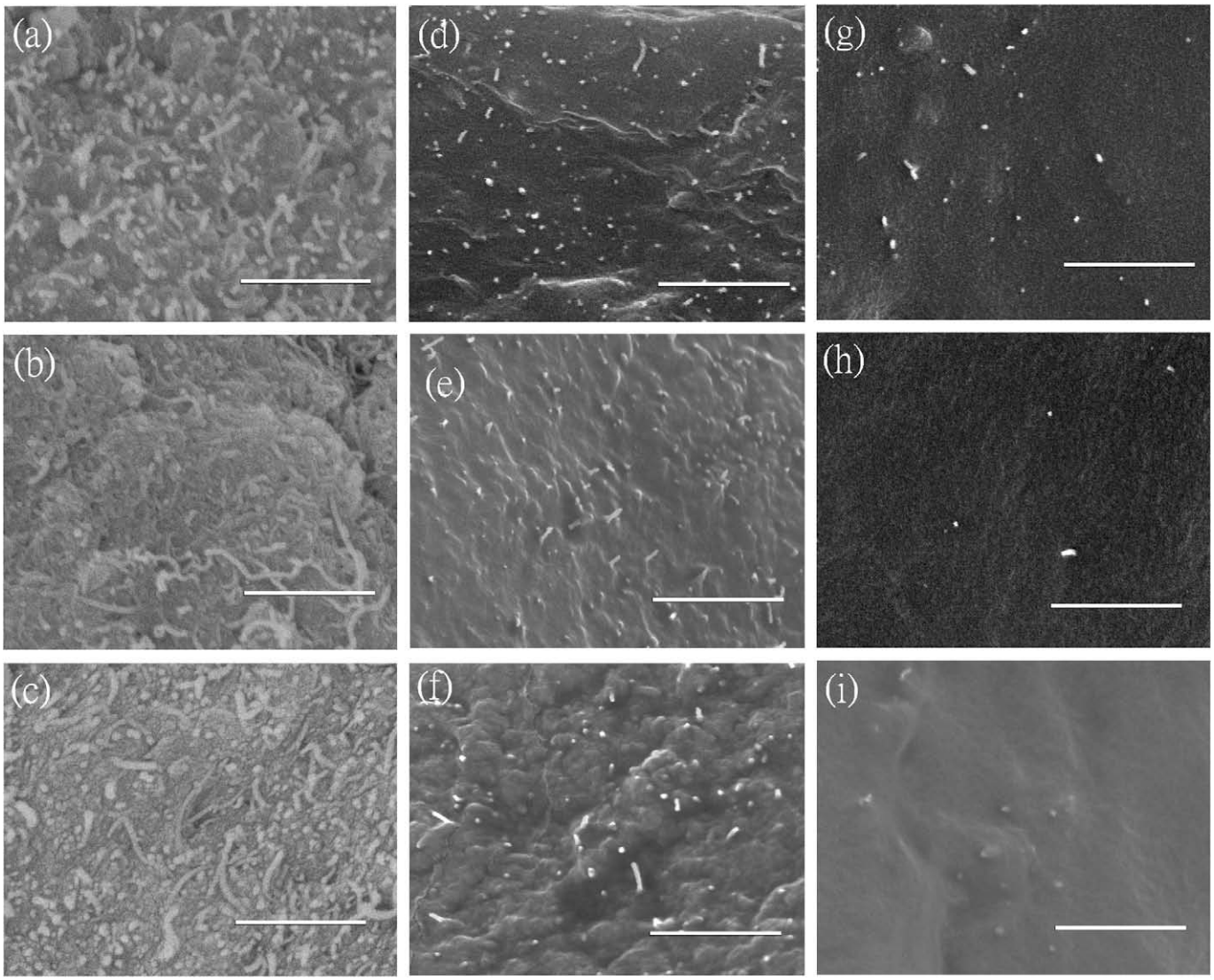

Fig. 6. SEM images (magnification: 20 k) of cross-sections of 20 wt.% MWCNT/PT derivative composite films: (a) pristine MWCNT/PDHOT, (b) pristine MWCNT/P(DHOT-*co*-DMOT), (c) pristine MWCNT/P3HT, (d) pristine MWCNT/PDHOT-DBSA, (e) pristine MWCNT/P(DHOT-*co*-DMOT)-DBSA, (f) pristine MWCNT/P3HT-DBSA, (g) MWCNT-HA/PDHOT-DBSA, (h) MWCNT-HA/P(DHOT-*co*-DMOT)-DBSA, (i) MWCNT-HA/P3HT-DBSA. (Scale bar: 1 μm.)

tween the CPs and the pristine MWCNTs resulted in effective dispersion, as a result of the PT derivatives wrapping around the pristine MWCNTs, they could not prevent the aggregation and entanglement of the pristine MWCNTs at higher fill contents. After we doped the PT derivatives with DBSA, however, the pristine MWCNTs exhibited different morphologies in the matrix (Fig. 6d–f). The aromatic ring of DBSA attached to the surface of the pristine MWCNTs through π–π interactions; its dodecyl chain had high compatibility with the alkyl or alkoxyl chains of the matrices. Thus, DBSA played two roles in this system: surfactant and doping agent. It not only increased the intrinsic conductivity of the PT derivatives but also provided more effective dispersion of the pristine MWCNTs. Therefore, the pristine MWCNTs were extended fully in each matrix—we did not observe any coiled pristine MWCNTs. Fig. 6g–i displays the morphologies of the composites obtained after replacing the pristine MWCNTs with MWCNT-HA. Unexpectedly, they exhibited a homogenous structure in which only a small amount of the free MWCNT-HA units were visible. This behavior presumably arose for two reasons: (a) the hexylbenzene groups increased the solubility of MWCNT-HA in $CHCl_3$, thereby overcoming the van der Waals interactions between the MWCNTs and resulting in their debundling; (b) the hexylbenzene groups formed well-packed structures with the side chains of DBSA and the PT derivatives. Thus, the MWCNT-HA units dispersed in each matrix existed in very small bundles, or even as isolated tubes.

Fig. 7 displays the electrical conductivities of the MWCNTs/PT derivatives. In general, when we added more MWCNTs to a matrix, the conductivity increased accordingly; the composites containing MWCNT-HA exhibited higher conductivities because of its more effective dispersion relative to that of the pristine MWCNTs. Nevertheless, the conductivity did not increase too dramatically because the MWCNTs (CP181) possessed a higher density of defects (Fig. 3). On the other hand, P3HT doped with DBSA provided the best conductivity in each PT derivative, due to its high crystallinity. For CPs such as PEDOT [23] and polyaniline [24], the crystalline region contains a well-ordered polymer chain structure. In this domain, interchain interactions are sufficiently strong to allow the charge to delocalize [25]. After adding the pristine MWCNTs or MWCNT-HA, the conductivity of the PDHOT composites extended beyond that of P3HT, possibly because the two hexyloxy chains of PDHOT enhanced its solubility and allowed the polymer to wrap

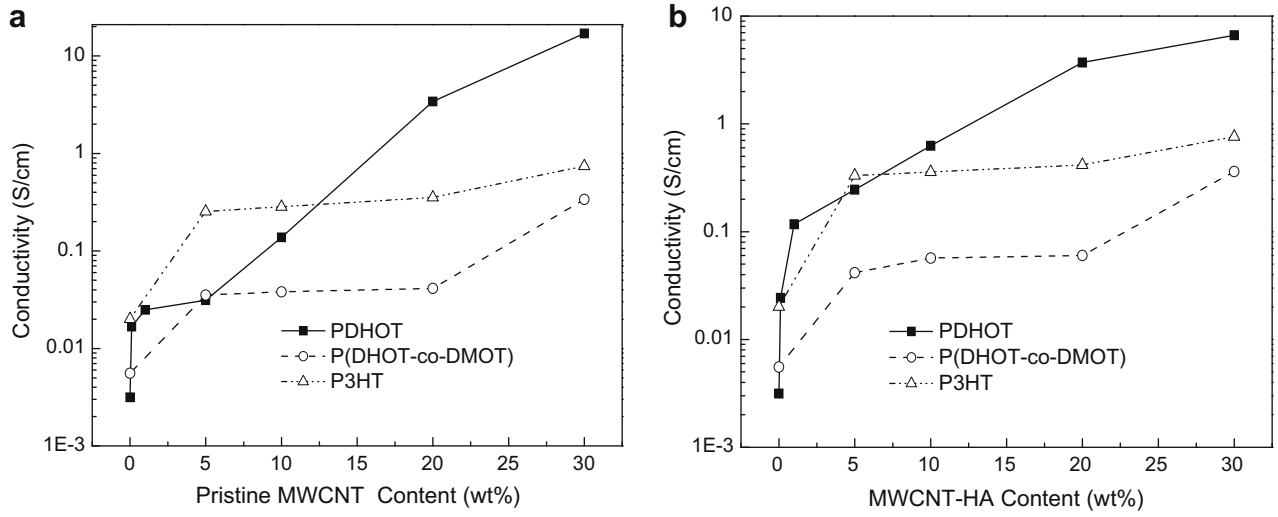

Fig. 7. Plots of the electrical conductivities of DBSA-doped PT derivative composites with respect to their concentrations of: (a) pristine MWCNTs and (b) MWCNT-HA.

around the surfaces of the MWCNTs more readily. In addition, the composite of PDHOT mixed with 30 wt.% pristine MWCNTs had a higher conductivity than that featuring MWCNT-HA, presumably as a result of the conductivity of the pristine MWCNTs (21 S/cm) being higher than that of MWCNT-HA (16 S/cm), because the chemical modification decreased the density of the graphite carbon of the latter species. Therefore, when a composite had a higher MWCNT-HA content, the nature of the composite tended toward that of MWCNT-HA, thereby limiting the critical properties of the composite at high MWCNT-HA contents.

4. Conclusion

The incorporation of alkoxyl groups at the 3- and 4-positions of the thiophene ring decreases the value of E_g of PT derivatives. Indeed, the derivatives PDHOT and P(DMOT-*co*-DHOT) exhibit a wider absorption range in their UV–Vis spectra. On the other hand, alkyl-modified MWCNT-HA not only exhibited increased stability in $CHCl_3$ (relative to that of the pristine MWCNTs) but also improved compatibility with PT derivatives. When we mixed the DBSA-doped PT derivatives with MWCNT-HA, the bundles of MWCNTs were separated into individual strands as a result of interactions between the alkyl and alkoxyl side chains. Therefore, the composites could incorporate higher contents of MWCNTs ($\geqq$20 wt.%) while exhibiting homogeneous structures. Of the tested PT derivatives, PDHOT exhibited higher compatibility with MWCNT-HA because its two hexyloxy chains enhanced its solubility and allowed the polymer to wrap around the surface of the MWCNTs more readily. The conductivities of the resulting MWCNTs/PDHOT blends were influenced dramatically by their MWCNT contents.

Acknowledgments

We thank the Ministry of Economic Affairs and National Science Council, Taiwan, for financial support through Grants 95-EC-17-A-08-S1-015 and 97-2218-E-002-012.

References

[1] Park JS, Ryu TI, Song M, Yoon KJ, Lee MJ, Shin IA, et al. Polym Sci Part A: Polym Chem 2008;46:6175.
[2] Koeppe R, Bossart O, Calzaferri G, Sariciftci NS. Advanced photon-harvesting concepts for low-energy gap organic solar cells. Sol Energy Mater Sol Cells 2007;91:986.
[3] Pomerantz M. Handbook of conducting polymers. 2nd ed. Marcel Dekker; 1998. p. 277.
[4] Kumar A, Bokria JG, Buyukmumcu Z, Dey T, Sotzing GA. Poly(thieno[3,4-b]furan), a new low band gap polymer: experiment and theory. Macromolecules 2008;41:7098.
[5] Chen WC, Jenekhe SA. Small-bandgap conducting polymers based on conjugated poly(heteroarylene methines). 2. Synthesis, structure, and properties. Macromolecules 1995;28:465.
[6] Bredas JL, Heeger AJ, Wudl F. Towards organic polymers with very small intrinsic band gaps. I. Electronic structure of polyisothianaphthene and derivatives. J Chem Phys 1986;85:4673.
[7] Hoogmartens I, Adriaensens P, Vanderzande D, Gelan J, Quattrocchi C, Lazzaroni R, et al. Low-bandgap conjugated polymers. A joint experimental and theoretical study of the structure of polyisothianaphthene. Macromolecules 1992;25:7347.
[8] Chen WC, Jenekhe SA. Small-bandgap conducting polymers based on conjugated poly(heteroarylene methines). 1. Precursor poly(heteroarylene methylenes). Macromolecules 1995;28:454.
[9] Kumar A, Buyukmumcu Z, Sotzing GA. Poly(thieno[3,4-b]furan). A new low band gap conjugated polymer. Macromolecules 2006;39:2723.
[10] Iijima S. Helical microtubules of graphitic carbon. Nature 1991;354:56.
[11] Skakalova V, Dettlaff-Weglikowska U, Roth S. Electrical and mechanical properties of nanocomposites of single wall carbon nanotubes with PMMA. Synth Met 2005;152:349.
[12] Gao J, Zhao B, Itkis ME, Bekyarova E, Hu H, Kranak V, et al. Chemical engineering of the single-walled carbon nanotube–nylon 6 interface. J Am Chem Soc 2006;128:7492.
[13] Oh J, Kozlov ME, Kim BG, Kim HK, Baughman RH, Hwang YH. Preparation and electrochemical characterization of porous SWNT–PPy nanocomposite sheets for supercapacitor applications. Synth Met 2008;158:638.
[14] Wu HL, Ma CC, Yang YT, Kuan HC, Yang CC, Chiang CL. Morphology, electrical resistance, electromagnetic interference shielding and mechanical properties of functionalized MWNT and poly(urea urethane) nanocomposites. J Polym Sci Part B: Polym Phys 2006;44:1096.
[15] Wang W, Fernando KAS, Lin Y, Meziani MJ, Veca LM, Cao L, et al. Metallic single-walled carbon nanotubes for conductive nanocomposites. J Am Chem Soc 2008;130:1415.
[16] Geng J, Kong BS, Yang SB, Youn SC, Park S, Joo T, et al. Effect of SWNT defects on the electron transfer properties in P3HT/SWNT hybrid materials. Adv Funct Mater 2008;18:2659.
[17] Liu Q, Mao J, Liu Z, Zhang N, Wang Y, Yang L, et al. A photovoltaic device based on a poly(phenyleneethynylene)/SWNT composite active layer. Nanotechnology 2008;19:115601.
[18] Palacios-Lidon E, Perez-Garcia B, Abellan J, Miguel C, Urbina A, Colchero J. Nanoscale characterization of the morphology and electrostatic properties of poly(3-octylthiophene)/graphite-nanoparticle blends. Adv Funct Mater 2006;16:1975.
[19] Warman JM, de Haas MP, Anthopoulos TD, De Leeuw DM. The negative effect of high-temperature annealing on charge-carrier lifetimes in microcrystalline PCBM. Adv Mater 2006;18:2294.
[20] Cheng F, Adronov A. Suzuki coupling reactions for the surface functionalization of single-walled carbon nanotubes. Chem Mater 2006;18:5389.
[21] Dyke CA, Tour JM. Solvent-free functionalization of carbon nanotubes. J Am Chem Soc 2003;125:1156.

[22] Mishra SP, Sahoo R, Ambade AV, Contractor AQ, Kumar A. Synthesis and characterization of functionalized 3,4-propylenedioxythiophene and its derivatives. J Mater Chem 2004;14:1896.
[23] Groenendaal LB, Jonas F, Freitag D, Pielartzik H, Reynolds JR. Poly(3,4-ethylenedioxythiophene) and its derivatives: past, present, and future. Adv Mater 2000;12(7):481.
[24] Liu CD, Lee SN, Ho CH, Han JL, Hsieh KH. Electrical properties of well-dispersed nanopolyaniline/epoxy hybrids prepared using an absorption-transferring process. J Phys Chem C 2008;112:15956.
[25] Prigodin VN, Epstein AJ. Nature of insulator–metal transition and novel mechanism of charge transport in the metallic state of highly doped electronic polymers. Synth Met 2002;125:43.